Measurements of Total Cross Sections for the Scattering of Potassium Atoms by Rare Gases

Isao KUSUNOKI

Department of Chemistry, Faculty of Science, Kyoto University, Sakyo-ku, Kyoto

(Received January 21, 1971)

Total cross sections for the scattering of potassium by He, Ne, Ar, Kr, and Xe have been measured in the thermal energy range. The velocity of potassium beam is selected by a velocity selector of a slotted disk type. To obtain accurate total cross sections, the pumping effect of a McLeod gauge for the pressure measurements, the fringe effect of the scattering chamber, corrections for angular resolution and for thermal motion of the target gases are taken into consideration. A new type of scattering chamber with a variable length is used to eliminate the error of the effective scattering path length. Velocity dependence of total cross sections has been obtained and glory undulations are observed for potassium-xenon systems. For argon, krypton, and xenon the van der Waals constants are calculated from the absolute total cross sections. The values of C_{K-Ar}, C_{K-Kr}, and C_{K-Xe} are 237, 354, and 535×10^{-60} erg·cm^6, respectively, and are in good agreement with the theoretical ones of Dalgarno and Davison. For neon the velocity dependence of the total cross section can not be explained by the van der Waals potential, $-C/r^s$, where $s=6$. For helium the correction factors for thermal motion of the scattering gas are large and the value of s for attractive potential can not be determined unambiguously.

It is well known that total collision cross sections measured by the scattering of molecular beams can afford an excellent means to study interatomic forces. In the thermal energy range the total cross sections are mainly governed by the long range van der Waals attraction, and the van der Waals constants can be determined by the measurements of the total cross sections.

In the molecular beam study, the total cross sections for scattering of potassium atoms by rare gases have been measured by many investigators[1] since the pioneering work of Rosin and Rabi.[2] The reason for this choice may be that potassium is the easiest to handle and detect as the beam material, and rare gases are also easy to handle as target gases experimentally and theoretically. Thus, the total cross section for scattering of potassium atoms by argon atoms has been regarded as a standard in this kind of experiment.

However, there are several sources of errors in the method of determination of the absolute total cross section, and the values published by different investigators did not always coincide. On the other hand, the method of data analysis has improved in the last decade, and many experimental results in the past have been become obsolete. The main reasons are as follows.

(1) The treatment of Berkling *et al.*[3] for correction of the velocity distributions of the beam and target gases is superior to that of Rosin and Rabi,[2] because the former takes into account the velocity dependence of the total cross sections. It is also evident that monochromatic beams used in recent studies are superior to thermal beams.

(2) In measuring the pressures of scattering gases with a McLead gauge, mercury drag effect must be taken into consideration.[4]

(3) The concept for angular resolution was improved by Kusch[5] and Busch,[6] and it has been recognized that the correction can not be ignored for beams of rectangular cross sections.

(4) To estimate the van der Waals constant from the total cross section, the Schiff and Landau-Lifshitz approximation formula[7] is superior to the Massey-Mohr formula.[8,9]

(5) There are few papers in which the effective scattering lengths are determined experimentally and unambiguously.

In a previous paper, the author took into consideration the above-mentioned items (1), (2), and (4).[10] In the present work, the absolute total cross sections for the scattering of potassium atoms by rare gases have been measured with the velocity selected beams, and the van der Waals constants have been estimated by the Schiff and Landau-Lifshitz approximation. Moreover, the effective scattering lengths have been determined experimentally, and other possible sources of error have also been taken into account.

Theoretical

For the measurement of the total collision cross section of gas molecules by means of the molecular beams, Beer's law is applicable for attenuation of the beam intensity, thus

$$I = I_0 \exp(-nQL), \quad (1)$$

where I_0 and I are the intensities of primary and at-

1) *Cf. e.g.*, a review by R. B. Bernstein and J. T. Muckerman, in "Intermolecular Forces" (Advances in Chemical Physics, Vol. 12), J. O. Hirschfelder, Ed., Interscience, New York (1967), Chap. 8.

2) S. Rosin and I. I. Rabi, *Phys. Rev.*, **48**, 373 (1935).

3) K. Berkling, R. Helbing, K. Kramer, H. Pauly, Ch. Schilier, and P. Toschek, *Z. Physik*, **166**, 406 (1962).

4) H. Ishii and K. Nakayama, *Trans. 8th Vacuum Symp. and 2nd Intern. Congress* (Pergamon Press, 1961) p. 519.

5) P. Kusch, *J. Chem. Phys.*, **40**, 1 (1964).

6) F. Busch, *Z. Physik*, **193**, 412 (1966).

7) L. I. Schiff, *Phys. Rev.*, **103**, 443 (1956); L. D. Landau and E. M. Lifshitz, "Quantum Mechanics", Pergamon Press, London (1959) p. 416.

8) H. S. W. Massey and C. B. O. Mohr, *Proc. Roy. Soc.*, **A144**, 188 (1934).

9) R. B. Bernstein and K. H. Kramer, *J. Chem. Phys.*, **38**, 2507 (1963).

10) I. Kusunoki, This Bulletin, **40**, 69 (1967).

tenuated beams, respectively. Q is the total cross section, L is the scattering path length, and n is the density of the target gas in the scattering chamber. Equation (1) is only correct for the ideal case in which a monochromatic molecular beam passes through a static target gas. However, as the target gas atoms are always moving, it is necessary to replace Eq. (1) by the equation

$$I = I_0 \exp(-nQ_{eff}L), \tag{2}$$

where Q_{eff} is an average total cross section over the whole relative velocity range. According to Berkling *et al.*,[3] the effective total cross section $Q_{eff}(v_i)$ at a beam velocity v_i, is related to the absolute total cross section $Q_i(v_i)$ as follows,

$$Q_0(v_i) = Q_{eff}(v_i)/Fa_0(s, x), \tag{3}$$

where $Fa_0(s,x)$ is a correction factor. Numerical values of $Fa_0(s,x)$ for $s=4$, 5, 6, and 7 have been calculated by a computer.[11] The values for $s=6$ coincide with those tabulated in Ref. 3.

All the apparatuses always have finite angular resolutions for detection of the scattering event. Thus, the scattering inside the resolving angle should be corrected. In the present experiment the beam and the detector have rectangular cross sections perpendicular to the direction of the beam, and their heights are larger than their widths. The angular resolution is not uniform, and depends on the position in the plane of the detector and the point in the scattering region. However, for a narrow rectangular beam it is expected to be uniform along its height.

Consider a particle scattered in the scattering chamber from a point at a distance l from the plane of the detector, and at a distance z from the vertical central line of the beam (Fig. 1). If the trajectories of the unscattered atoms are sufficiently parallel to each other, a part of the beam scattered through an angle Θ and falls on the detector is given by

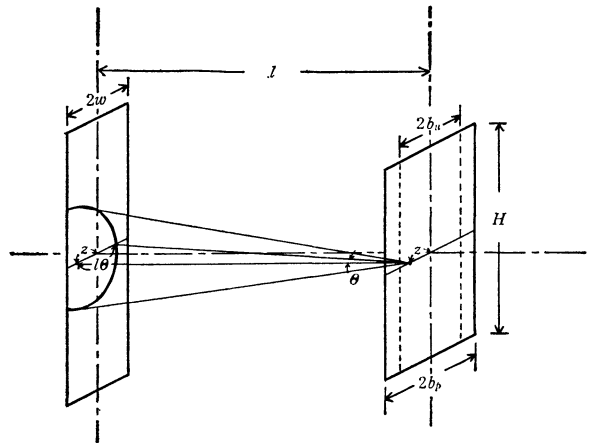

Fig. 1. Geometrical parameters for the correction of angular resolution.

$$2\pi ni(z)R(z, l, \Theta)\sigma(\Theta)\sin\Theta d\Theta, \tag{4}$$

where n is the density of the scattering gas, $i(z)$ is the beam intensity at the scattering point, $R(z,l,\Theta)$ is the portion of the circumference of the circular cone of the scattered beam intercepted by the detector, and $\sigma(\Theta)$ is the differential cross section in the laboratory system.[12]

In the first approximation the correction term for angular resolution is obtained in the case of $z=0$ and $l=$constant, thus

$$\Delta Q(v_i) = 2\pi\int_0^{\pi} R(l, \Theta)\sigma(v_i, \Theta)\sin\Theta d\Theta \tag{5}$$

A formula representing a more perfect correction for the angular resolution is

$$\Delta Q(v_i) = \frac{2\pi\int_{l_{cd}-L}^{l_{cd}}\int_{-b_p}^{b_p}\int_0^{\pi} i_0(z)e^{-nQ(l_{cd}-l)}R(z, l, \Theta)\sigma(v_i, \Theta)\sin\Theta d\Theta dz dl}{\int_{l_{cd}-L}^{l_{cd}}\int_{-b_p}^{b_p} i_0(z)e^{-nQ(l_{cd}-l)}dz dl}, \tag{6}$$

where l_{cd} is the distance from the entrance slit of the scattering chamber to the detector, b_p is the half width of penumbra of the beam profile at the scattering plane, and L is the effective length of the scattering chamber.

We previously assumed a beam of infinite height, but in this experiment a beam of finite height is used. Thus the R-function has to be modified to a function of h, and Eq. (6) becomes

$$\Delta Q(v_i) = \frac{2\pi\int_{-H}^{H}\int_{l_{ed}-L}^{l_{cd}}\int_{-b_p}^{b_p}\int_0^{\pi} i_0(z)e^{-nQ(l_{cd}-l)}R(h, z, l, \Theta)\sigma(v_i, \Theta)\sin\Theta d\Theta dz dl dh}{2H\int_{l_{cd}-L}^{l_{cd}}\int_{-b_p}^{b_p} i_0(z)e^{-nQ(l_{cd}-l)}dz dl}, \tag{7}$$

where $2H$ is the height of the beam. However, in the experiment h is much larger than b_p (*i.e.* $H\sim100\ b_p$), and the R-function is nearly independent of h over the whole region of h. Therefore, the final correction term can be given by Eq. (6). Unfortunately, n and Q are included in Eq. (6), and a calculation of the equation is intractable. If the distance l_{cd} is much larger than L, the correction term may be simplified to

$$\Delta Q(v_i) = \frac{2\pi\int_{-b_p}^{b_p}\int_0^{\pi} i_0(z)R(z, \Theta)\sigma(v_i, \Theta)\sin\Theta d\Theta dz}{\int_{-b_p}^{b_p} i_0(z)dz}. \tag{8}$$

However, if b_p is larger than the half width of the detector w, there are some parts of the beam which do not contribute to I_0, but some atoms scattered from these parts fall on the detector. In such a case, the integral region of z in the denominators of Eqs. (6—8) should be from $-w$ to w.

The correction values can be calculated by a computer, but the calculation is troublesome. In the present case, Busch's method[6] seems to be satisfactory

11) These values will be published elsewhere.

12) The procedure to obtain $\sigma(\Theta)$ from $\sigma(\theta)$ in the center-of-mass system will be given elsewhere.

and will be used.

Experimental

Figure 2 shows a schematic drawing of the apparatus, which consists of an oven chamber, a velocity selector chamber, and a measuring chamber. A scattering chamber and a beam detector are placed in the measuring chamber. In each chamber a liquid-nitrogen cooled plate to remove the surplus beam atoms is equipped. The chambers are pumped by 4-inch oil diffusion pumps with cold traps, typical operating pressures in these chambers being about 2×10^{-7} Torr. The pressures are kept constant during an experimental run.

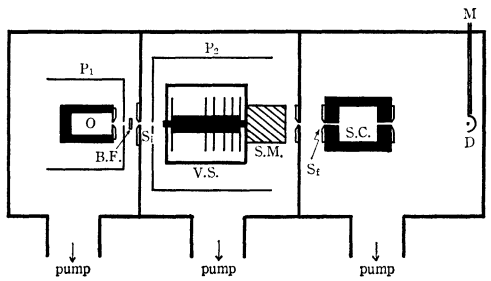

Fig. 2. Diagram of the beam apparatus. Drawing is not to scale. The labeled parts are: O, oven; B.F., beam flag; S_1, the first collimating slit; S_f, the final collimating slit; S.C., scattering chamber; D, detector; M, manipulator; $P_{1,2}$, liquid nitrogen cooled shields; V.S., velocity selector; S.M., synchronous motor.

Source. The oven is single chamber type and beam atoms effuse from a slit of 0.19 mm width. It is made of stainless steel and supported by three tungsten pins on a movable plate with dove-tails. The heater current of the oven is supplied by a DC power stabilizer. The temperature of the oven is measured by a chromel-alumel thermocouple, and the beam intensity is monitored by a surface ionization gauge in front of the source.

Velocity Selector. The velocity selector[13] is a slotted disk type. The number of disks is six and its total length L is 12.02 cm. The phase angle φ_0 is 0.2097 rad. and the velocity of the selected beams is given by

$$v = \frac{\omega L}{\varphi_0} = 360f \text{ (cm/sec)}, \tag{9}$$

where ω is the angular velocity of the rotating disks and f is the number of revolutions per second. The thickness of the disks is 3 mm, which is thicker than those used by the others.[14] However, the slits are cut obliquely along the beam path and its transmission is 47.6%. The width of the slits is 0.50 mm and the mean width of each tooth is 0.505 mm. The number of these slits or teeth is 360 per disk of diameter 12.5 cm. The length of slits in the radial direction is 5 mm. The resolution of the selector ($\Delta v/v$) is 3.96%. The selector is driven by a synchronous motor (Electronic Specialty Co. EF17H71). Power is supplied to the motor from a two-phase oscillator (NF circuit design block Co.). The number of revolutions of the selector is monitored by reflected light pulses from the disk surface painted with black stripes by a photomultiplier and a frequency counter.

13) K. Kodera and I. Kusunoki, *Oyobutsuri* (in Japanese), **38**, 20 (1969).

14) H. U. Hostettler and R. B. Bernstein, *Rev. Sci. Instrum.*, **31**, 872 (1960); S. M. Trujillo, P. K. Rol, and E. W. Rothe. *ibid.*, **33**, 841 (1962).

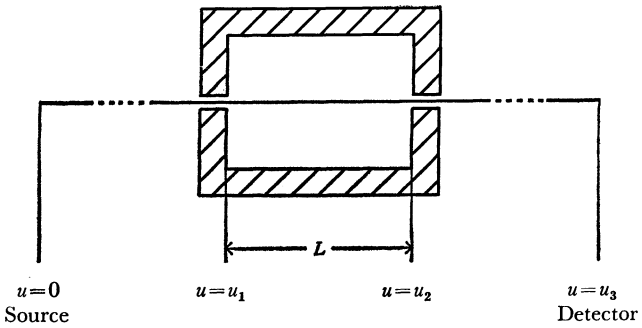

Fig. 3. Conventional scattering chamber.

Scattering Chamber. A conventional scattering chamber is shown in Fig. 3. Scattering gas in the chamber effuses out along the beam path. Thus, the effective path length L_{eff} for the beam attenuation can be given by

$$n_0 L_{eff} = \int_0^{u_1} n(u)\mathrm{d}u + n_0 L + \int_{u_2}^{u_3} n(u)\mathrm{d}u, \tag{10}$$

where n_0 is the number density of gas molecules inside the chamber, L is the inside length, and $n(u)$ is the density along the beam path. Rothe *et al.*[15] have driven an approximate formula for the estimation of L_{eff}, but a reliable estimation of $n(u)$ is not easy.

To avoid uncertainty of estimation by an approximate formula and obtain an exact value of n_0L, a chamber with a variable length, as shown in Fig. 4, is used. The chamber

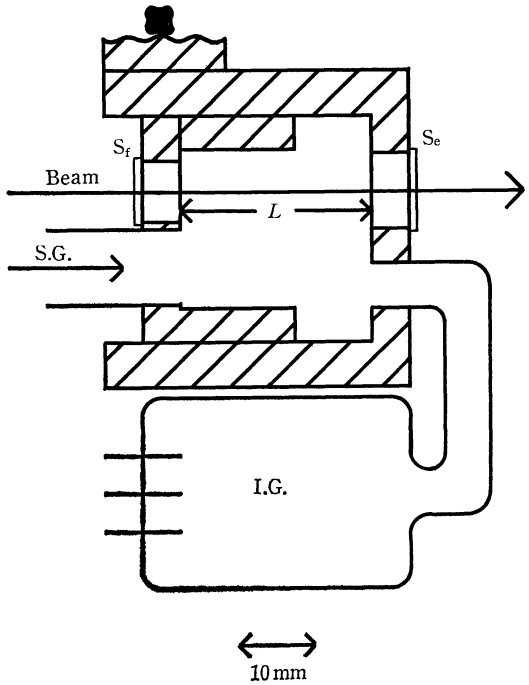

Fig. 4. Vertical cross section of the scattering chamber. S_f, entrance slit; S_e, exit slit; S.G., scattering gas; I.G., ionization gauge.

consists of two cylinders; one slides inside the other and the length of the chamber can be changed from 15 mm to 30 mm. Operation can be performed from outside the vacuum vessel. The dimensions of entrance and exit channels and slits are: channels:

15) E. W. Rothe, L. L. Marino, R. H. Neynaber, P. K. Rol, and S. M. Trujillo, *Phys. Rev.*, **126**, 598 (1962).

widths, 1.0 mm
heights, entrance 8 mm, exit 10 mm
lengths, 5.0 mm
slits:
widths, entrance 0.06 mm, exit 0.35 mm
heights, entrance 8 mm, exit 10 mm.
The entrance slit functions as a collimating slit in this beam system.

The scattering chamber is evacuated by a Hickman oil diffusion pump, and the scattering gases are introduced into the chamber from a gas reservoir through a glass capillary.

Detector. In order to detect the potassium beam, a Langumuir-Taylor surface ionization detector is used. The filament is biased by +90 V relative to the ion collector. Ion current is measured with a vibrating-reed electrometer and recorded by a two-pen recorder along with the pressure in the scattering chamber.

Angular Resolution. The distance from the source slit to the collimating slit l_{sc} is about 70 cm, and the distance from the collimating slit to the detector l_{cd} is 10.5 cm. The angle subtended by the collimating slit at the position of the source slit is 8.6×10^{-5} rad. Thus, trajectories of the atoms in the beam are almost parallel to each other. The angle subtanded by the collimating slit at the detector is 5.7×10^{-4} rad. The angle subtended by the detector at the scattering center, previously taken as a geometrical resolution, is 4.1×10^{-4} rad. The geometrical half width of the umbra of unscattered beam profile b_u is 0.02 mm, and that of the penumbra b_p is 0.049 mm. According to Kusch's criterion[5] the angular resolution determined by the beam profile is 4.0×10^{-4} rad.

Pressure Measurement. To determine the absolute cross section, the most important and the most difficult problem is to measure the absolute pressure of target gases. In the present experiment a large McLeod gauge calibrated in our laboratory by mercury weighing, is used as a standard pressure gauge. The McLeod gauge is similar to that of Rosenberg[16] and the gauge constant is 3.32×10^{-7} (*i.e.* $P=3.32\times h^2\times10^{-7}$ Torr, h in mm). With this large volume gauge the absolute pressures of the rare gases in the range of 5×10^{-5} to 5×10^{-4} Torr can easily be measured. However, it is not suitable to measure the pressure in the scattering chamber directly by the McLeod gauge, because the connecting tube between the chamber and the gauge becomes so long that a pressure gradient may arise between them, and furthermore, it can not measure the pressure continuously.

To measure the pressure of the rare gases in the scattering chamber an ionization gauge (Mitsubishi K-30) is connected directly to the scattering chamber with a short glass tube and placed in the measuring chamber. The tube is bent in order to prevent the gas from passing through it without collisions with the wall. This caution is necessary, because the temperature of the scattering gas should be equal to that of the wall anywhere in the chamber.

The sensitivities of the ionization gauge for rare gases are calibrated by the McLeod gauge described above. For calibration of the sensitivities the mercury drag effect has to be considered, because the mercury vapor stream from the McLeod gauge to the cold trap inserted between the ionization gauge and the McLeod gauge brings about an error in the absolute pressure measurement. The magnitude of the effect depends on the ambient temperature, the tubing diameter and length, the gas pressure, and the diffusion constant of the gas in mercury vapor. According to Takaishi,[17] the effect is estimated by the expression

$$\frac{P''-P'}{P'}=\frac{P_{Hg}}{P'}\left\{1-\frac{1}{B}\ln\left(\frac{P''}{P'}\right)\right\},$$

$$B=3\alpha^2\sigma^2\{m_g/(m_g+m_{Hg})\}^{1/2}rP_{Hg}/4kT \qquad (11)$$

where P' and P'' are the pressure of the gas in a McLeod gauge and that of the gas to be calibrated, respectively. P_{Hg} is a pressure of the mercury vapor at the temperature of T. $\pi\sigma^2$ is a collisional cross section between the mercury atom and a gas atom; m_g and m_{Hg} are the molecular weights of the gas and mercury, r is a radius of the connecting tube ($r=$ 0.4 cm), and α is a constant about 1.[18] To eliminate the effect completely, the cut-off position of the McLeod gauge is cooled with dry ice in order to remove the mercury vapor stream as described by Ishii and Nakayama.[4]

The sensitivities of the ionization gauge measured for rare gases are given in Table 1. The relative sensitivities are compared with the values of other authors. The present values determined by cooling the cut-off position are close to those of Rothe,[19] obtained by placing the McLeod gauge in a refrigerator to get rid of the mercury drag effect. On

TABLE 1. SENSITIVITIES OF IONIZATION GAUGE FOR RARE GASES AND RELATIVE SENSITIVITIES TO ARGON

	X				
	He	Ne	Ar	Kr	Xe
Sensitivity, *SA*	2.87±0.06	4.80±0.07	23.6±0.5	34.1±0.8	48.5±0.4
SA_X/SA_{Ar}	0.122	0.204	1.00	1.45	2.06
Sensitivity, *SB*	2.91	5.00	26.0	40.0	59.0
SB_X/SB_{Ar}	0.112	0.192	1.00	1.54	2.27
SB_X/SA_X-1	0.01	0.04	0.10	0.17	0.22
B (at $T=295$°K)	0.023	0.055	0.097	0.145	0.190
$P''/P'-1$ (at $P'<1\times10^{-4}$ Torr)	0.02	0.05	0.10	0.16	0.21
Relative sensitivities to argon in other papers.					
Duschman and Young[19]	0.13	0.20	1.00	1.56	2.29
Rothe[20]	0.128	0.221	1.00	1.40	2.02

SA: Sensitivity calibrated by the McLeod gauge whose cut-off position is cooled with Dry Ice.
SB: Sensitivity calibrated by the McLeod gauge without consideration of the mercury drag effect.

16) P. Rosenberg, *Rev. Sci. Instrum.*, **10**, 131 (1939).
17) T. Takaishi, *Trans. Faraday Soc.*, **61**, 840 (1965).
18) Y. Sensui, private communication.
19) E. W. Rothe, *J. Vac. Sci. Technol.*, **1**, 66 (1964).

Table 2. Total cross sections at v_k = 720 m/sec

	He			Ne		Ar	Kr	Xe
Q_{eff}(Å²)	359±9			282±20		500±18	576±23	672±23
s	5	6	7	4	6	6	6	6
$Fa_0(s, x)$	1.27	1.47	1.54	1.056	1.117	1.059	1.027	1.018
Q_0	260	242	231	267	252	473±17	561±22	661±28
Q_w						505±18	602±24	714±30

the other hand, the values obtained without cooling are close to those of Dushman and Young,[20] in which no precaution against the effect has been taken. The magnitude of the effect is expressed by a factor $SB/SA-1$. As shown in Table 1, the values are in good agreement with those calculated with Takaishi's theory.

Results

The effective total cross section Q_{eff} is usually obtained by

$$I = I_0 \exp(-n_0 L_{eff} Q_{eff}) \tag{12}$$

where $n_0 L_{eff}$ is a value given by Eq. (10). If the beam attenuation is measured at different scattering lengths, the fringe effective represented by the first and third terms of Eq. (10) may be compensated, and the effective total cross section can be estimated by the equation

$$Q_{eff} = \frac{1}{L_1 - L_2}\left\{\left[\frac{\ln(I_0/I)}{n}\right]_1 - \left[\frac{\ln(I_0/I)}{n}\right]_2\right\} \tag{13}$$

where suffixes 1 and 2 refer to the values of different lengths of the scattering chamber, and L_1 and L_2 represent the inside lengths of the chamber without the channel region. During the measurement it is very difficult to change the length keeping the pressure constant, because the outgas from the wall by changing the length disturbs the pressure of the scattering chamber. A typical result is shown in Fig. 5 for the scattering of the velocity selected potassium beam (720 m/sec) by xenon with L=20, 25, and 30 mm. Using Eq. (13), Q_{eff} is estimated from the slopes of the lines as

$$Q_{eff}(720\ \text{m/sec}) = 672\ \text{Å}^2.$$

Results for all the rare gases are shown in Table 2.

The effective scattering length L_{eff} is also estimated from Fig. 5 by the equation

$$(L_i)_{eff} = \frac{1}{Q_{eff}}\left[\frac{\ln(I_0/I)}{n}\right]_i, \tag{14}$$

where Q_{eff} is a value obtained by Eq. (13). The effective scattering length obtained for various scattering gases are plotted in Fig. 6 against the geometrical length of the scattering chamber. The effective length L_{eff} is calculated for L_1=30 mm. Open circles are the values measured with the thermal beams, and solid circles are those measured with the velocity selected beams (720 m/sec). All the values fall within the range of 40.0±0.7 mm which is nearly equal to the length of the scattering chamber including channels at both ends. The value calculated by the equation

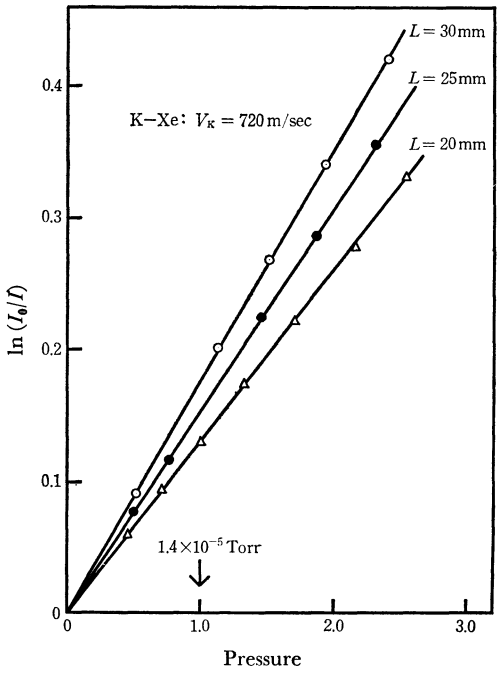

Fig. 5. Attenuation of potassium beam *vs.* pressure of xenon gas. L is the length inside the scattering chamber.

derived by Rothe *et al.*, shown by an arrow $\bar{A}$, is 38.4 mm, while $\bar{B}$ is the value calculated by the following equation derived by the author.

$$(L_i)_{eff} = \frac{l}{2}\left[1 + \frac{8Ka^2b}{8Ka^2b + 3(a+b)lc}\right] + L_i + \frac{l'}{2}\left[1 + \frac{8K'a'^2b'}{8K'a'^2b' + 3(a'+b')l'c'}\right], \tag{15}$$

where a, b, and l are the width, height, and length of the entrance channel, respectively, K its Clausing factor and c the width of the entrance slit; a', b', l', and K' are the corresponding quantities for the exit channel, and c' of the exit slit. In this case, the value of $(L_1)_{eff}$ amounts to 39.0 mm. Both of the calculated values are smaller than the experimental values, which are independent of the gaseous species and the beam velocity. Therefore, L_{eff}=40.0 mm is used in Eq. (12) to estimate Q_{eff}.

The absolute total cross section, $Q_0(v_i)$, may be obtained from $Q_{eff}(v_i)$ by means of Eq. (3). However, to estimate an accurate absolute total cross section, a correction for angular resolution has to be considered. Calculations of the correction described in the theoretical section are complicated and troublesome. In the present analysis, the Busch approximation for argon, krypton, and xenon is used because the discrepancy

20) S. Dushman, "Scientific Foundations of Vacuum Technique," John Wiley, & Sons, Inc., New York, London (1962), p. 324.

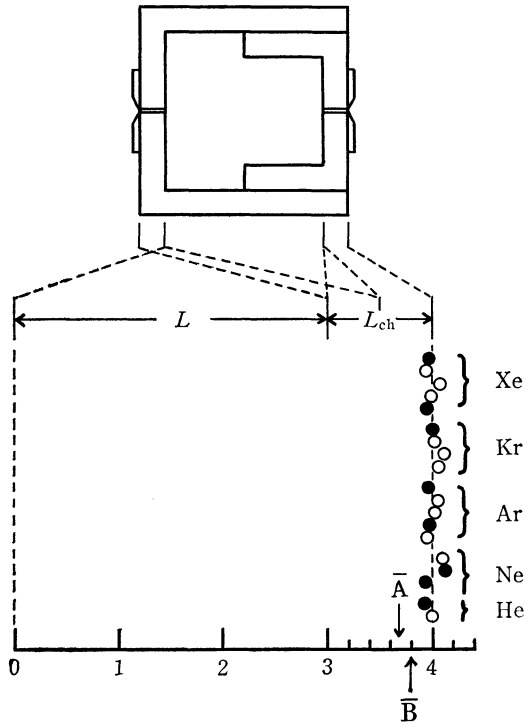

Fig. 6. Effective scattering lengths measured by rare gases. L_{ch}, length of channel region; ○, measured by thermal beam; ●, measured by the velocity selected beam.

from the exact calculation should be small. The correction factor[21] is given by

$$\frac{dQ}{Q} = 0.0765\sqrt{Q_0 k_i^2}\gamma\left(1 + \frac{0.368}{x^2}\right), \qquad (16)$$

$$\gamma = \frac{b_u + b_p}{l} \quad \text{for } w \leq b_p.$$

Then, the corrected absolute total cross section Q_w is calculated by

$$Q_w = \frac{Q_0}{(1 - dQ/Q)}. \qquad (17)$$

The correction amounts to 5-10%. In Table 2 the corrected total cross sections Q_0 and Q_w are listed for the beam velocity of 720 m/sec, which corresponds approximately to the most probable beam velocity and is obtained from 200 rps of the velocity selector. Figure 7 shows the variations in the total cross section Q_w for K–Ar, K–Kr, and K–Xe systems against the velocity of the potassium beam in a logarithmic scale. The straight lines with slopes of −2/5 correspond to $s=6$. For argon an agreement with $s=6$ is fairly good. The slopes of these curves for krypton and xenon are slightly steeper than −2/5. This means that s is smaller than 6, and between 5 and 6. This may be due to the glory effect or some unknown systematic experimental error. As the temperature of the scattering chamber is relatively high (*i.e.* room temperature), no undulation of the total cross section

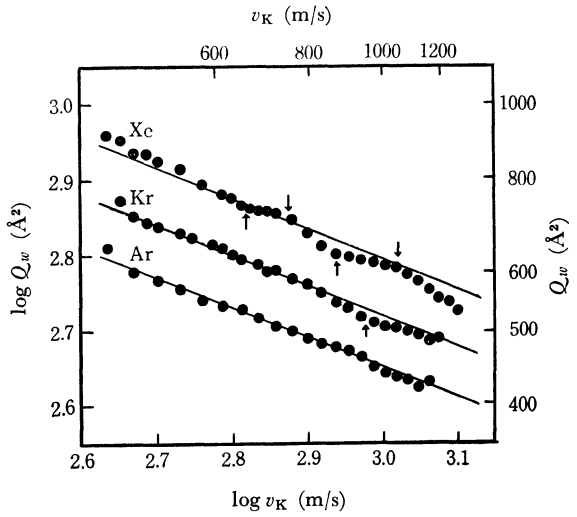

Fig. 7. log Q_w *vs.* log v_K plots for K-Ar, K-Kr, and K-Xe systems. Arrows show the positions of extrema.

is obtained for argon. However, a trace of undulation can be observed for krypton, and a more definite undulation for xenon.

For neon and helium similar treatments are not feasible, because it is not clear whether the interatomic potential can be approximated by a simple attraction with $s=6$ in the measured velocity range. For neon log Q_{eff} *vs.* log v_K plots are in Fig. 8. In this case, even after the correction with $Fa_0(6, x)$ a large discrepancy remains between the theoretical and the experimental curves. However, the values corrected with $Fa_0(4, x)$ are in fair agreement with the slope of $s=4$. The correction for angular resolution will give a less steep slope than that of the plotted values and results in a better agreement. For helium, log Q_{eff} *vs.* log v_K plot and the corrected values with $Fa_0(5, x)$, $Fa_0(6, x)$, and $Fa_0(7, x)$ are shown in Fig. 9. In this correction, factors of Fa_0 are very large, and it is not clear which correction is the best.

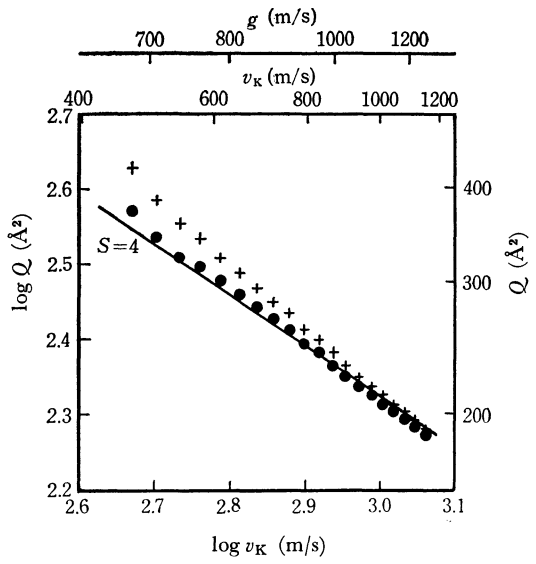

Fig. 8. log Q_{eff} and log Q_0 *vs.* log v_K plots for K-Ne system. +, data of Q_{eff}; ●, data of Q_0 corrected with $Fa_0(4, x)$.

21) F. Busch, H. J. Strunck, and Ch. Schlier, *Z. Physik*, **199**, 518 (1967).

Discussion

The relation between the total cross section and the van der Waals constant is given by

$$Q(v) = p\left[\frac{C}{\hbar v}\right]^{2/5}, \tag{18}$$

where p is a dimensionless constant. It is 8.083 according to the SLL aproximation.

The van der Waals constants calculated from the total cross sections are listed in Table 3. C is a mean value over the measured velocities. The values of the present work are smaller than the experimental values of other authors. However, the values for argon, krypton, and xenon are in good agreement with recent theoretical values, being slightly smaller. For the K–Ar system, the discrepancies of our value with the theoretical one of Dalgarno and Davison[28] and with that of Mahan[29] are within 10%, which is within experimental uncertainty. The relative values of C for argon C_X/C_{Ar} are in good agreement with those of Dalgarno and Davison. For neon and helium, the van der Waals constants can not be derived from the experimental values of total cross sections, because in these cases interatomic interactions may not purely be those of a van der Waals nature.

From the glory undulation of the velocity dependence of the total cross section, the value of εr_m can be estimated. According to Bernstein and O'Brien,[30] the extremum condition can be given by

$$N - \frac{3}{8} = \frac{2\varepsilon r_m a_1}{\pi\hbar v_N}\left[1 - \frac{A_1\varepsilon}{a_1 E_N} + \frac{A_2\varepsilon^2}{a_1 E_N{}^2}\right], \tag{19}$$

where $A_1=0.1625$, $A_2=0.0801$, a_1 is a known function of κ which is the curvature at the potential minimum, N is the index number of the extremum, and E_N is

Table 3. Van der Waals constants (10^{-60} erg·cm^6)

	K-Ar	K-Kr	K-Xe
Exporimental			
Florin[22]	280		740
Helbing-Pauly[23]	410		1070
Lulla *et al.*[24]	572		
Rothe-Neynaber[25]	300	500	
Brooks[26]	294		
Kusunoki[10],[a]	250	340	530
present work	237	354	535
(C_{K-X}/C_{K-Ar})	(1.00)	(1.49)	(2.26)
Theoretical			
Dalgarno-Kingston[27]	267	400	648
Dalgarno-Davison[28]	260	380	600
	(1.00)	(1.46)	(2.30)
Mahan[29]	254	377	610

a) Previous values are reestimated from the total cross sections corrected with the angular resolution.

Table 4. Potential parameters obtained by various investigators

	potential	K-Kr			K-Xe			method
		εr_m 10^{-22} erg·cm	ε 10^{-14} erg	r_m Å	εr_m 10^{-22} erg·cm	ε 10^{-14} erg	r_m Å	
Beck[31]	Exp-6, for $\alpha=12$		1.24	6.0				r
Rothe *et al.*[32]	L-J (8,6)	6.88	1.30	5.29				u
Hundhausen-Pauly[33]	L-J (12,6)					1.52	9.4	r
	L-J (8,6)					1.81	7.3	
Beck-Loesch[34]	L-J (12,6)	7.62	1.3	5.85	11.9	2.5	4.75	u
	L-J (8,6)	6.83	1.5	4.55	10.7	3.0	3.6	
Busch *et al.*[21]	L-J (8,6)	6.84			10.6			u
Hollstein-Pauly[35]	L-J (12,6)	7.8			12.1			u
	L-J (8,6)	7.0			10.8			
Buck-Pauly[36]	(11,44 ; 84,6)		1.42	5.24		2.20	5.25	s. c.
Düren *et* al.[37]	9-parameters		1.45	4.84				s. c.
present work	L-J (12,6)	(8.0)	(1.7)	(4.67)	11.0	2.3	4.76	u
	L-J (8,6)	(7.2)	(1.7)	(4.13)	9.9	2.5	4.0	

r, rainbow effect, u, undulation of total cross section, s. c., semiempirical calculation.

22) H. Florin, Diplom Thesis, University of Bonn, (1964).
23) R. Helbing and H. Pauly, *Z. Physik*, **179**, 16 (1964).
24) K. Lulla, H. H. Brown, and B. Bederson, *Phys. Rev.*, **136**, A1233, (1964).
25) E. W. Rothe and R. H. Neynaber, *J. Chem. Phys.*, **42**, 3306, 4178 (1965).
26) P. R. Brooks, *Bull. Am. Phys. Soc.*, **10**, 382 (1965).
27) A. Dalgarno and A. E. Kingston, *Proc. Roy. Soc.* (London), **73**, 455 (1959).
28) A. Dalgarno and W. D. Davison, *Advan. At. Mol. Phys.*, **2**, 1 (1966).
29) G. D. Mahan, *J. Chem. Phys.*, **48**, 950 (1968).
30) R. B. Bernstein and T. J. P. O'Brien, *ibid.*, **46**, 1208 (1967).
31) D. Beck, *ibid.*, **37**, 2884 (1962).
32) E. W. Rothe, R. H. Neynaber, B. W. Scott, S. M. Trujillo, and P. K. Rol, *ibid.*, **39**, 493 (1963).
33) E. Hundhausen and H. Pauly, *Z. Physik*, **187**, 305 (1965).
34) D. Beck and H. J. Loesch, *ibid.*, **195**, 444 (1966).
35) M. Hollstein and H. Pauly, *ibid.*, **201**, 10 (1967).
36) U. Buck and H. Pauly, *ibid.*, **208**, 390 (1968).
37) R. Düren, G. P. Raabe, and Ch. Schlier, *ibid.*, **214**, 410 (1968).

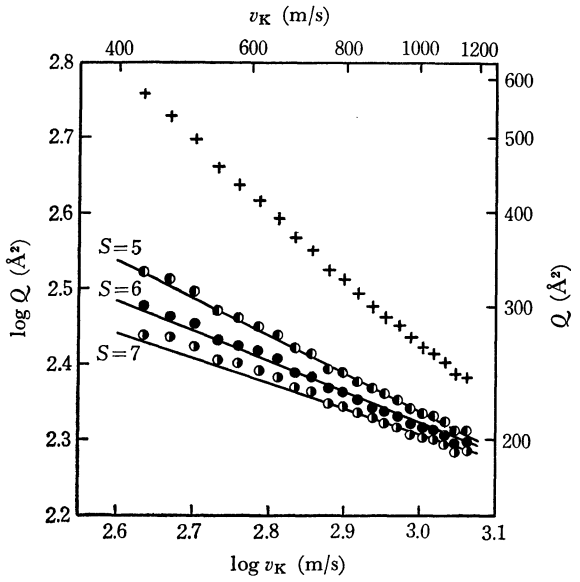

Fig. 9. log Q_{eff} and log Q_0 *vs.* log v_K plots for K-He system.
◐, corrected with Fa_0 (5, x); ●, corrected with $Fa_0(6, x)$; ◑, corrected with $Fa_0(7, x)$; +, data of Q_{eff}.

$1/2\,\mu v_N^2$. In the present work, the velocities of a maximum and a minimum for K–Xe system are around 1040 m/sec and 870 m/sec, respectively. According to Beck and Loesch,[34] these values correspond to v_N for $N=3$ and 3.5. Thus, for the L-J(12, 6) potential the value $\varepsilon r_m = 11.0\times10^{-22}$ erg·cm is obtained. Similarly, the value $\varepsilon r_m = 8.0\times10^{-22}$ erg·cm is obtained for K–Kr system. If the L–J(8, 6) potential is assumed instead of the L–J(12,6) potential, the values εr_m are smaller than those for L–J(12, 6) potential, as shown in Table 4. However, these values may contain errors of about 10%, because the undulation is obscured by the thermal motion of target gases.

For the L–J(12, 6) potential, the van der Waals constant C is equal to $2\,\varepsilon r_m^6$. Then, if the values of εr_m are combined with the experimental values of C, ε, and r_m can be estimated separately. These values are listed in Table 4.

For the K–Ne or K–He system, the values of εr_m are unknown, but they may be smaller than 4.5×10^{-22} erg·cm for K–Ar system.[34] If the value of $\varepsilon r_m/\hbar g$ is less than 3—5, there is no extremum given by Eq. (19), and the velocity dependence of the total cross section is not represented adequately by Eq. (18).[38] In the present study, the values of $\hbar g$ for these systems are larger than 0.7×10^{-22} erg·cm. Therefore, if the value εr_m is smaller than 2.5×10^{-22} erg·cm, the above condition may be satisfied, and the velocity range will correspond to the transition range from the predominantly attractive $s=6$ to the predominantly repulsive $s=12$ ranges.

The present work was partly supported by the Toray Science Foundation. The author would like to thank Professor Kumasaburo Kodera for his valuable advice and guidance. The assistance of Mr. Atsuhiro Sakiyama during the course of the experiment is also acknowledged.

38) *Cf. e.g.*, a review by R. B. Bernstein, in "Molecular Beams" (Advances in Chemical Physics, Vol. 10), J. Ross, Ed., Interscience, New York (1966), Chap. 3.